Electron-impact rotationally elastic total cross sections for H_2CO and $HCOOH$ over a wide range of incident energy (0.01–2000 eV)

Minaxi Vinodkumar,[1,*] Harshad Bhutadia,[2] Bobby Antony,[3] and Nigel Mason[4]

[1]*V P & R P T P Science College, Vallabh Vidyanagar 388 120, Gujarat, India*
[2]*Government Engineering College, Patan 384265, Gujarat, India*
[3]*Department of Applied Physics, Indian School of Mines, Dhanbad JH-826004, India*
[4]*Department of Physics & Astronomy, Open University, Milton Keynes MK7 6AA, United Kingdom*

This paper reports computational results of the total cross sections for electron impact on H_2CO and $HCOOH$ over a wide range of electron impact energies from 0.01 eV to 2 keV. The total cross section is presented as sum of the elastic and electronic excitation cross sections for incident energies. The calculation uses two different methodologies, below the ionization threshold of the target the cross section is calculated using the UK molecular R-matrix code through the QUANTEMOL-N software package while cross sections at higher energies are evaluated using the spherical complex optical potential formalism. The two methods are found to be consistent at the transition energy ($\sim$15 eV). The present results are, in general, found to be in good agreement with previous experimental and theoretical results (wherever available) and, thus, the present results can serve as a benchmark for the cross section over a wide range of energy.

PACS number(s): 34.80.Bm

I. INTRODUCTION

The study of radiation damage to living tissues, including DNA, has been a major topic of research in the medical sciences for nearly a century since the damaged DNA can mutate and ultimately lead to the development of a cancer. However, a more detailed understanding of radiation damage at the molecular level has only recently been developed. For example, only recently has the role of DNA damage by secondary electrons been quantified. A pioneering study by Boudaiffa *et al.* [1] showed that low-energy electrons can break the single and/or double strand of DNA by the process of dissociative electron attachment (DEA). Thereafter, low-energy DEA studies have been found to have a significant role in radiation physics and the need to study electron interactions with biomolecules has been highlighted [2]. The present study is a preliminary attempt toward the investigation of electron interactions with larger biomolecules, since, although formaldehyde and formic acid are not themselves major biomolecules, they play a key role in the formation of more pertinent compounds such as acetic acid and glycine, while the formate group (-COOH) is a key component in many amino acids.

The search for prebiotic molecules beyond the solar system, especially in the interstellar medium, is one of the most exciting topics for astrochemistry since, if found, their presence would suggest that the "ingredients" of life are common to star and planet formation and, hence, life may have the opportunity to develop in many "solar systems" and is not restricted to the special conditions on Earth. To date, technology has restricted most observational studies to the simpler precursor molecules [3–5], including formaldehyde (H_2CO) [6,7]. However, the recent detection of traces of the simplest amino acid, glycine (NH_2CH_2COOH) in the interstellar medium [8] has stimulated the astrochemistry community to focus on this area of research further and the observation of larger more complex molecules will be a major objective of the new ALMA telescope array, including the search for larger amino acids (it being noted that more than 50 different amino acids have been detected in meteorites [9]) and simple acids such as formic acid. The presence of double hydrogen bonds in both formaldehyde and formic acid makes these studies still more interesting since these hydrogen bonds serve as a model system for the understanding of DNA base pairs [8] providing a possible mechanism for a larger-scale macromolecule assembly. Multiple proton transfer in H-bonded species is one of the fundamental molecular mechanisms in biology, as it governs oxidation-reduction steps in many reactions; indeed, various gas-phase synthetic routes have been suggested [9] for the formation of different molecules from these simple precursors by electron interaction. Hence, low and intermediate energy electron collision studies on these interstellar molecules are required.

Considerable progress has been made in the study of electron-molecule collision studies in the past decade both experimentally and theoretically. By utilizing better electron spectrometers and adopting position-sensitive detectors, experimentalists can produce accurate cross-sectional data on electron collisions with larger molecules and even explore free radical species. However, given the vast number of molecular systems and the requirement for an ever-increasing amount of data, the experimental community cannot meet the demands of the myriad of data users. Accordingly, we must look to theory to provide much of the required electron-scattering data. On the theoretical front, with the advent of high-performing computers and the development of very accurate theories, computation of reliable cross-section data is now possible at least for smaller targets but since these detailed computational methods are computationally taxing and require long time scales (the study of one or two molecular targets is common in many Ph.D. programs) there is a need for more generic and faster (if more approximate) calculations to provide data to the user community on their time scales (often weeks or, at most, months).

_____

*minaxivinod@yahoo.co.in

At low electron impact energies (<10 eV) short-lived anions (resonances) may be formed which may then subsequently decay to produce neutral and anionic fragments. This will highly influence the local chemistry. Hence, the prediction of low-energy resonance formation, which is strongly linked with the forces acting on the electrons during the scattering process and, therefore, the structural properties of the target, can be of at the utmost importance in understanding local chemistry. Alternatively, intermediate- to high-energy electron-scattering cross sections are required in other fields like astrophysics, atmospheric physics, and radiation physics, where high-energy radiations x rays, cosmic rays, and so on, interact with a range of targets. These high-energy interactions can produce an avalanche of secondary electrons which then provide the lower-energy electrons for further chemical reactions. Consequently, there is a need for electron impact total scattering cross sections over a wide energy range from meV to MeV.

In this article we present electron impact total cross section, Q_T, data for formaldehyde (H_2CO) and formic acid (HCOOH) over a wide energy range from 0.01 eV to 2 keV. Q_T is presented as a sum of the elastic and electronic excitation cross sections for incident energies. Below the ionization threshold of the target the cross sections are calculated using the UK molecular R-matrix code through the QUANTEMOL-N software package (Q_{mol}) while cross sections at higher energies are evaluated using the spherical complex optical potential formalism. The two methods are found to be consistent at the transition energy ($\sim$15 eV). The present results are, in general, found to be in good agreement with previous experimental and theoretical results (wherever available) and, thus, the present results can serve as a benchmark for the cross section over a wide range of energy.

Despite the importance of formaldehyde in medicine and astrophysics, there are only a few previous electron impact collision studies. The latest theoretical work for electron impact elastic integral, differential, and momentum transfer cross sections for formaldehyde is that of Kaur and Baluja [10] using the R-matrix code to study electron interactions between 0.01 and 20 eV. We have previously reported total elastic, total ionization, and total cross section for formaldehyde by employing a group additivity rule using the spherical complex optical potential (SCOP) formalism for impact energies beyond the ionization threshold of the target [11]. Surprisingly, there appears to be no theoretical or experimental work reporting total cross sections for this molecule. Hence, the data may be used as a benchmark for the user community.

Compared to formaldehyde, formic acid has been studied more extensively. Recent experimental work by Vizcaino *et al.* [12] has reported a set of differential cross sections for elastic scattering in the energy range 1.8 to 50 eV and deduced integral and momentum transfer cross sections from these results. Total scattering measurements were performed by Kimura *et al.* [13] in the low-energy range 0.1–60 eV. Theoretical calculations have been reported by Gianturco and Lucchese [14] locating resonant states at low energies. We have also reported total elastic, total ionization, and total cross sections using the group additivity rule for impact energies beyond the ionization threshold of the target [11]. In this paper, we report cross sections spanning the low- and high-energy regions.

II. THEORETICAL METHODOLOGY

This paper reports low-energy (0.01 eV to about 15 eV) *ab initio* calculations using Q_{mol} [15] which utilizes the UK molecular R-matrix code [16] while the SCOP method is employed for calculating total (elastic plus inelastic) cross sections beyond the ionization threshold up to 2 keV [17]. As these two are very different formalisms we will discuss them separately in the following two subsections; however, first, we will discuss the target model employed.

A. Target model

H_2CO is a trigonal planar molecule with bond angle of 116.5° between HCH. We have used a double ζ plus polarization (DZP) Gaussian basis set for our target wave-function representation. The double ζ basis set is important because it allows us to treat each orbital separately when we conduct the Hartree-Fock calculation. This gives us a more accurate representation of each orbital. Care has been taken to restrict the basis set within the R-matrix radius by not using a very big basis set with diffused functions. H_2CO has a C_{2V} point group symmetry of the order 4. The Hartree-Fock electronic configuration of the ground state is $1a_1^2, 2a_1^2, 3a_1^2, 4a_1^2, 1b_2^2, 5a_1^2, 1b_1^2, 2b_2^2$. Of a total of 16 electrons, we have frozen 4 electrons in two molecular orbitals (viz. $1a_1, 2a_1$) while 12 electrons are kept in the active space of nine molecular orbitals ($3a_1, 4a_1, 5a_1, 6a_1, 7a_1, 1b_1, 2b_1, 1b_2, 2b_2$). A total of eight target states are represented by 696 configuration state functions (CSF's) for the ground state and the number of channels included in the calculation is 150. The GAUSPROP and DENPROP modules [18] yield a ground-state energy of −113.92 Hartree which is in very good agreement with the values of Pulay *et al.* [19], Sobrinho *et al.* [20], Sun *et al.* [21], and Kaur and Baluja [22], as shown in Table I. The present computed dipole moment in the equilibrium geometry is 1.0086 a.u., which is very close to the experimental values of Shoolery and Sharbaugh [23] and values from Ref. [24] and the theoretical values of Ref. [24], Kaur and Baluja [22], Sun *et al.* [21], and Sobrinho *et al.* [20]. The present calculated first electronic excitation energy is 4.44 eV which finds excellent agreement with the theoretical data of Kaur and Baluja [22] and in Refs. [20,21,25–27]. The rotational constant obtained in the present calculation is 9.406 cm^{-1} and is also in excellent agreement with experimental and theoretical data from the National Institute of Standards and Technology (NIST) [24]. The electronic excitation thresholds for formaldehyde are listed in Table II.

HCOOH is a planar molecule with the OCO angle equal to 123° [28]. We have used a double ζ plus polarization (DZP) basis set for our calculations. HCOOH has a C_S point group symmetry of the order 2. The Hartree-Fock electronic configuration of the ground state is $1a_1^2, 2a_1^2, 3a_1^2, 4a_1^2, 5a_1^2, 6a_1^2, 7a_1^2, 8a_1^2, 1a_2^2, 9a_1^2, 2a_2^2, 10a_1^2$. Of a total of 24 electrons, we have frozen 6 electrons in three molecular orbitals (viz. $1a_1, 2a_1, 3a_1$) while 18 electrons are kept in active space within 11 molecular orbitals ($4a_1, 5a_1, 6a_1, 7a_1, 8a_1, 9a_1, 10a_1, 11a_1, 1a_2, 2a_2, 3a_2$). The total number of generated CSF's for the ground state is 642 and the number of channels included in the calculation is 100. The Hartree-Fock calculation yields a ground-state energy of −188.82 Hartree

TABLE I. Properties of molecular targets H_2CO and H_2CO_2: Ground-state energy (Hartree), dipole moment (a.u.), first excitation energy (eV), and rotational constant (cm^{-1}).

Target	Ground-state energy (Hartree)		Dipole moment (a.u.)			First excitation energy E_1 (eV)		Rotational constant (B) (cm^{-1})		
	Present	Theor.	Present	Theor.	Expt.	Present	Theor.	Present	Theor.	Expt.
H_2CO	-113.92	-113.89 [22]	1.0086	1.04 [24]	0.917 [24]	4.44	4.54 [22]	9.406	9.74 [24]	9.40 [24]
		-113.89 [21]		1.04 [22]	0.912 [23]		3.41 [25]			
		-113.90 [20]		1.08 [21]			3.46 [26]			
		-113.90 [19]		1.10 [20]			4.14 [27]			
							4.08 [21]			
							4.09 [20]			
H_2CO_2	-188.82	-188.83 [28]	0.5718	0.551 [24]	0.555 [24]	6.26	$-$	2.607	2.68 [24]	2.58 [24]

which is again in excellent agreement with the theoretical values of Gianturco and Lucchese [29]. The present dipole moment of 0.5718 a.u. agrees well with the experimental value given by NIST [24]. We report seven electronic excitation states for formic acid (see Table II) with the first electronic excitation energy calculated as 6.26 eV. To the best of our knowledge there are no data, either theoretical or experimental, for the first electronic energy reported in the literature. The present computed rotational constant 2.607 cm^{-1} is also in good agreement with experimental and theoretical values in the NIST database [24].

B. Low-energy formalism (0.01 ∼ 15 eV)

The R-matrix method [16] splits configuration space into an inner region, which is a sphere of radius "a" about the target's

TABLE II. Vertical excitation energies of excited states of H_2CO and H_2CO_2 (in eV).

H_2CO		HCOOH	
State	Energy (eV)	State	Energy (eV)
$^3A''$	4.44	$^3A''$	6.26
$^1A''$	4.76	$^1A''$	6.57
$^3A'$	6.50	$^3A'$	7.30
$^3B'$	9.51	$^1A'$	9.88
$^1B'$	10.16	$^3A''$	10.29
$^3B''$	10.24	$^3A'$	10.38
$^3A''$	10.84	$^1A''$	10.82
$^3B''$	10.94		
$^1A''$	11.04		
$^1A'$	11.46		
$^1B''$	11.63		
$^1A'$	12.19		
$^3B'$	14.30		
$^1B'$	14.58		
$^3A'$	15.00		
$^3B''$	15.88		
$^3A'$	16.12		
$^3A''$	16.30		
$^1B''$	17.09		
$^1A''$	17.36		

center of mass, and an outer region. The inner region is usually chosen to have a radius of around 10 a.u. and the outer region of about 100 a.u.. The choice of this value depends on the stability of the results obtained in the inner region and outer region calculation and is an effect of the extent of electronic charge density distribution around the center of mass of the target. Presently, we have taken 10 a.u. as the inner R-matrix radius which was found to give consistent results.

In the inner region the total wave function for the system is written as [16],

$$\psi_k^{N+1} = A \sum_I \psi_I^N (x_1, \cdots, x_N) \sum_j \zeta_j(x_{N+1})a_{Ijk}$$
$$+ \sum_m \chi_m(x_1, \cdots, x_{N+1})b_{mk}, \quad (1)$$

where A is the antisymmetrization operator, x_N is the spatial and spin coordinate of the nth electron, ξ_j is a continuum orbital spin-coupled with the scattering electron, and a_{Ijk} and b_{mk} are variational coefficients determined in the calculation. The first summation runs over the target states used in the close-coupled expansion. The second summation runs over configurations χ_m, where all electrons are placed in target molecular orbitals. The number of these configurations varies considerably with the model employed. With the wave function given by Eq. (1), a static exchange calculation has a single Hartree-Fock target state in the first sum. The second sum runs over the minimal number of configurations usually 3 or fewer, required to relax orthogonality constraints between the target molecular orbitals and the functions used to represent the configuration. Our fully close-coupled calculation uses the lowest number of target states, themselves represented by a configuration interaction (CI) expansion in the first expansion and over 100 configurations in the second. These configurations allow for both orthogonality relaxation and short-range polarization effects. It should be noted that with CI target representations, the distinction between which configurations represent which of these effects becomes blurred.

The target and the continuum orbitals here are represented by Gaussian-type orbitals (GTOs) and the molecular integrals are generated by the appropriate molecular package. The R matrix will provide the link between the inner region and outer region. For this purpose, the inner region is propagated to the outer region potential until its solutions match with

the asymptotic functions given by the Gailitis expansion [16]. Thus, by generating the wave functions, using Eq. (1), their eigenvalues are determined. These coupled single-center equations describing the scattering in the outer region are integrated to identify the K-matrix elements. Consequently, the resonance positions, widths, and various cross sections can be evaluated using the T matrix obtained from the S matrix which is, in turn, obtained from the K-matrix elements.

C. Higher-energy formalism (15 eV–2 keV)

High-energy electron scattering is modeled using the SCOP formalism [30,31] which employs partial-wave analysis to solve the Schrödinger equation with various potentials as its input. The electron-molecule system can be represented by a complex potential comprising real and imaginary parts as

$$V_{\text{opt}}(r, E_i) = V_R(r) + i V_I(r, E_i) \qquad (2)$$

such that

$$V_R(r, E_i) = V_{\text{st}}(r) + V_{\text{ex}}(r, E_i) + V_p(r, E_i), \qquad (3)$$

where E_i is the incident energy. Equation (2) corresponds to various real potentials to account for the electron target interaction, namely static, exchange, and the polarization potentials, respectively. These potentials are obtained using the molecular charge density of the target, the ionization potential, and polarizability as inputs. We describe the scattering within the fixed-nuclei approximation which neglects any dynamics involving the nuclear motion (rotational as well as vibrational), whereas the bound electrons are taken to be in the ground electronic state of the target at its optimized equilibrium geometry. The molecular charge density may be derived from the atomic charge density by expanding it from the center of mass of the system. Depending on the size of the molecule more than one center may be conceptualized and, hence, calculations are performed using the total charge density obtained by adding these various centers of charge density, after normalizing them to account for the total number of electrons present. The atomic charge densities and static potentials (V_{st}) are formulated from the parameterized Hartree-Fock wave functions given by Cox and Bonham [32].

Hara's "free electron gas exchange model" [33] is used for the exchange potential (V_{ex}). The polarization potential (V_p) is formulated from the parameter free model of correlation-polarization potential given by Zhang *et al.* [34]. Here, various multipole nonadiabatic corrections are incorporated in the intermediate region which will approach the correct asymptotic form at large "r" smoothly. The target parameters such as the ionization potential (IP) and dipole polarizability (α_o) of the target we used are the best available from literature [35].

The imaginary part in V_{opt} called the absorption potential V_{abs} will account for the total loss of flux scattered into the allowed electronic excitation or ionization channels. The expressions used here are vibrationally and rotationally elastic. This is due to the fact that these nonspherical terms do not contribute much to the total potential at the present high-energy range.

The well-known quasifree model form of Staszeweska *et al.* [36] is employed for the absorption part and is given by

$$V_{\text{abs}}(r, E_i) = -\rho(r)\sqrt{\frac{T_{\text{loc}}}{2}}\left(\frac{8\pi}{10k_F^3 E_i}\right)$$
$$\times \theta(p^2 - k_F^2 - 2\Delta)(A_1 + A_2 + A_3). \quad (4)$$

Where the local kinetic energy of the incident electron is

$$T_{\text{loc}} = E_i - (V_{\text{st}} + V_{\text{ex}} + V_p) \qquad (5)$$

and where $p^2 = 2E_i$, $k_F = [3\pi^2\rho(r)]^{1/3}$ is the Fermi wave vector and A_1, A_2, and A_3 are dynamic functions that depends differently on $\theta(x)$, I, Δ, and E_i. Here, I is the ionization threshold of the target, $\theta(x)$ is the Heaviside unit step function and Δ is an energy parameter below which $V_{\text{abs}} = 0$. Hence, Δ is the principal factor which decides the values of total inelastic cross section, since below this value ionization or excitation is not possible. This is one of the main characteristics of Staszewska model [36]. We have modified this model by considering Δ as a slowly varying function of E_i around I. Such an approximation is meaningful since Δ fixed at I would not allow excitation at energies $E_i \leqslant I$. However, if Δ is much less than the ionization threshold, then V_{abs} becomes unexpectedly high near the peak position. This amendment yields a reasonable minimum value $0.8I$ to Δ and also to express the parameter as a function of E_i around I, i.e.,

$$\Delta(E_i) = 0.8I + \beta(E_i - 1). \qquad (6)$$

Here the value of the parameter β is obtained by requiring that $\Delta = I$(eV) at $E_i = \text{E}_p$, the value of incident energy at which Q_{inel} reaches its peak. E_p can be found by calculating Q_{inel} by keeping $\Delta = I$. Beyond E_p, Δ is kept constant and is equal to I. The expression given in Eq. (6) is such that if Δ is fixed at the ionization potential, it would not allow any inelastic channel to open below I; also, if it is very much less than I, then V_{abs} becomes significantly high close to the peak position of Q_{inel}.

The complex potential thus formulated is used to solve the Schrödinger equation numerically through partial-wave analysis. This calculation will produce complex phase shifts for each partial wave which carries the signature of interaction of the incoming projectile with the target. At low energies only a few partial waves are significant, but as the incident energy increases more partial waves are needed for convergence. The phase shifts (δ_l) thus obtained are employed to find the relevant cross sections, total elastic (Q_{el}), and the total inelastic cross sections (Q_{inel}) using the scattering matrix $S_l(k) = \exp(2i\delta_l)$ [37]. The total scattering cross section (TCS), Q_T [38], then is found by adding these two cross sections together.

III. RESULTS AND DISCUSSION

The present work reports total cross sections for e–H_2CO and e–HCOOH scattering. We have employed the *ab initio* R-matrix code below the ionization threshold of the target. The total cross section is sum of total elastic and total electronic excitation cross sections below ionization threshold of the target. Above ionization threshold of the target we have computed the total cross section as the sum of total elastic and total inelastic cross section using the SCOP formalism. The

TABLE III. Total electron-scattering cross sections of H_2CO and H_2CO_2 ($Å^2$).

Energy (eV)	Cross sections	
	H_2CO	HCOOH
0.1	570.00	580.40
0.2	270.00	336.45
0.4	131.00	198.45
0.6	89.30	148.23
0.8	71.00	121.44
1.0	63.50	104.44
1.5	66.40	80.10
2.0	42.30	67.17
3.0	26.80	61.37
4.0	22.80	49.00
5.0	21.50	40.61
6.0	21.10	36.60
7.0	20.80	34.15
8.0	20.60	32.61
9.0	20.30	31.57
10	20.00	30.69
11	19.70	29.67
12	19.30	28.78
13	19.00	27.93
14	18.50	27.03
15	18.10	27.80
20	15.50	29.15
30	13.77	27.49
40	13.28	25.85
80	10.58	17.90
100	09.64	16.28
200	06.76	11.88
300	05.53	09.43
400	04.75	07.81
500	04.18	06.66
600	03.74	05.80
700	03.39	05.13
800	03.11	04.60
900	02.87	04.17
1000	02.66	03.82
1500	01.97	02.67
2000	01.57	02.04

data sets produced by two formalisms are consistent at the transition energy (~15 eV). This was also observed in the case of CH_4, SiH_4 [39], NH_3, H_2S, and PH_3 [40]. All the numerical results of total cross section (in $Å^2$) for both the targets from 0.1 to 2000 eV are presented in the Table III and are also represented graphically in Figs. 1 and 2.

Figure 1 compares the presently calculated total cross section for e–H_2CO scattering with previous data where available. As can be seen from the graph that there is very smooth transition between the data computed using R-matrix code and SCOP formalism. As discussed earlier there is only one theoretical work reported by Kaur and Baluja [22] using the R-matrix code from 0.1 to 20 eV. The present data shows a broad resonance peak at 1.46 eV which is very close to the resonance peak computed at 1.32 eV by Kaur and Baluja [22] (Table IV). These resonances are reflected in total cross section as a peak in the cross section. The present data and data of Kaur
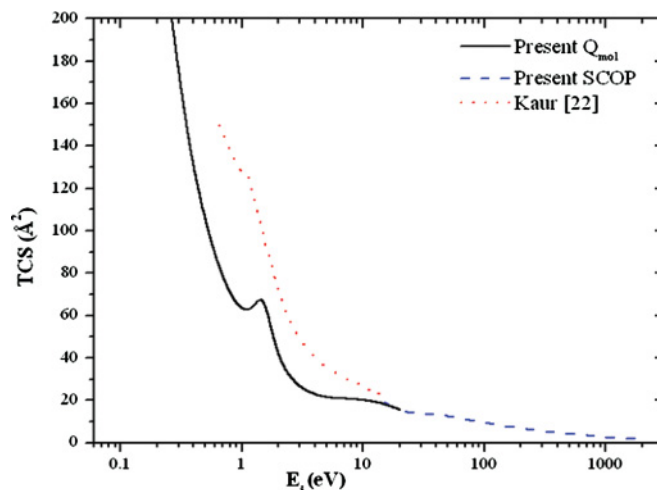
FIG. 1. (Color online) Total cross sections for e–H_2CO scattering in $Å^2$. (Solid line) Present Q_{mol}; (dashed line) present SCOP; (dotted line) Kaur and Baluja [22].

and Baluja [22] show similar trends, with any differences in the two data sets being attributed to different representation of target wave function.

Figure 2 compares our present e–HCOOH scattering results with other available data. In contrast to H_2CO, HCOOH has been studied by many groups at low energies [12–14]. A major theoretical study has been made by Gianturco et al. [14] to compute the total elastic cross section from 0 to 20 eV; however, they did not take into account the asymptotic polarizability in the full expansion of interaction potential. This may be the reason for their lower total cross sections at low energies compared to the present results. We have used partial waves up to $l = 4$ with higher partial waves computed using the Born approximation. The rapid rise in the cross section at low energy is attributed to the high dipole moment (1.0086 a.u.) of ground-state HCOOH. The present results and the results of Gianturco and Lucchese [14] both suggest a peak
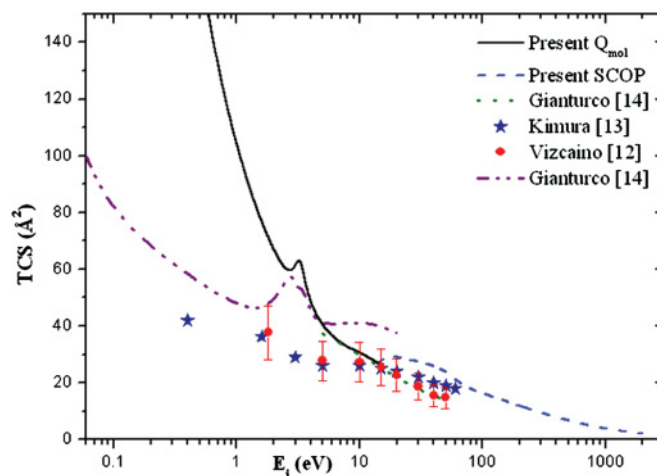
FIG. 2. (Color online) Total cross sections for e–HCOOH scattering in $Å^2$. (Solid line) Present Q_{mol}; (dashed line) present SCOP; (dotted line) Gianturco and Lucchese [14]; (dash-dot-dot line) Gianturco and Lucchese [14]; (star) Kimura et al. [13]; (filled circle) Vizcaino et al. [12].

TABLE IV. Comparison for resonance positions and widths for both H_2CO and HCOOH (in eV).

Target	Resonance positions			Resonance widths		
	Present	Theor.	Expt.	Present	Theor.	Expt.
H_2CO	1.46	1.32 [22]		0.794	0.546 [22]	–
HCOOH	3.23	3.49 [14]	1.25 [29]	0.95	0.93 [14]	–

in the cross section around 3 eV. There is a further systematic theoretical study carried out by Gianturco and Lucchese [29] to locate the resonance position. Accordingly they predict resonance at 3.49 eV with a narrow width of 0.93 eV which matches with present value of resonance at 3.23 eV with a narrow width of 0.95 eV as shown in Table IV. The present data are higher than the experimental data of Kimura *et al*. [13] below 10 eV due to Born correction, while above it they compare well with present results. Vizcaino *et al*. [12] have measured differential cross sections for elastic scattering and then derived integral cross sections for incident energies from 10 to 50 eV, the present results are also in excellent agreement with their derived cross sections above 10 eV. Below 10 eV neither Kimura *et al*. nor Vizcaino *et al*. appear to detect the resonance but this may be due to the incremental energy step in each of these experiments (which is large) and the difficulty in measuring differential cross sections at low energies (<5 eV). Nevertheless, it does suggest that the calculations may overestimate the cross section at low energy and in order to resolve this discrepancy further experiments are urgently needed.

The dependence of the rate coefficients with temperature for H_2CO and HCOOH, respectively, may also be derived from this data and, for electron mean energies below threshold, the rate coefficient increases rapidly with temperature or energy for both the systems.

IV. CONCLUSION

Electron impact studies of formaldehyde and formic acid have gained prominence due to the possible detection of such molecules in astrophysical environments since they are considered to be the primary constituents for the formation of larger amino acids and thus may play a role in the evolution of life. They are also important in developing models of electron

scattering from larger biomolecules which may be damaged by secondary electrons during irradiation (e.g., in cancer therapy). In this paper we have reported the total electron scattering cross section for these molecules using two formalisms. At low impact energies (up to the ionization threshold of the target) the *ab initio R*-matrix method was utilized through QUANTEMOL-N software while at high energies (beyond the ionization threshold of the target) we have employed the SCOP formalism. The data computed using two formalisms are consistent with a smooth transition around ~15 eV. The present data for total cross section is generally in good agreement with previous data (where available). This combination of these two formalisms can, therefore, produce a robust set of data when used in tandem (Table III). Moreover, the computed target properties such as ground-state energy, first electronic excitation energy, dipole moment, and rotational constant are found to agree well with the predicted theoretical and experimental results as evident from Table I. In Table II we have reported 20 electronic excitation energy states for H_2CO and seven electronic excitation energy states for formic acid. We have also observed formation of electron scattering resonances in both targets. For formaldehyde the present prediction of a resonance centred at 1.46 eV is very close to that predicted by Kaur and Baluja [22] at 1.32 eV. Similarly in formic acid the present prediction of a resonance at 3.46 eV is very close to the theoretical prediction of Gianturco and Lucchese [29] at 3.32 eV.

[1] B. Boudaiffa, P. Cloutier, D. Hunting, M. A. Huels, and L. Sanche, Science **287**, 1658 (2000).

[2] A. Pelc, A. Sailer, P. Scheier, M. Probst, N. J. Mason, E. Illenberger, and T. D. Mark, Chem. Phys. Lett. **361**, 277 (2002).

[3] B. E. Turner, Astrophys. J. Suppl. Ser. **76**, 617 (1991).

[4] Nummelin *et al*., Astrophys. J. Suppl. Ser. **128**, 213 (2000).

[5] D. M. Mehringer, L. E. Snyder, Y. Miao, and F. M. Lovas, Astrophys. J. **480**, L71 (1997).

[6] L. E. Snyder *et al*., Phys. Rev. Lett. **22**, 67 (1969).

[7] V. I. Goldanskii, Nature **268**, 612 (1977).

[8] F. A. Gianturco, R. R. Lucchese, J. Langer, I. Martin, M. Stano, G. Karwasz, and E. Illenberger, Eur. Phys. J. D **35**, 417 (2005).

[9] W. T. Huntress Jr. and G. F. Mitchell, Astrophys. J. **231**, 456 (1979).

[10] S. Kaur and K. L. Baluja, J. Phys. B: At. Mol. Opt. Phys. **38**, 3917 (2005).

[11] M. Vinodkumar, K. N. Joshipura, C. Limbachiya, and N. J. Mason, Phys. Rev. A **74**, 022721 (2006).

[12] V. Vizcaino, M. Jelisavcic, J. P. Sullivan, and S. J. Buckman, New J. Phys. **8**, 8 (2006).

[13] M. Kimura, O. Sueoka, A. Hamada, and Y. Itikawa, Adv. Chem. Phys. **111**, 537 (2000).

[14] F. A. Gianturco, R. R. Lucchese, J. Langer, I. Martin, M. Stano, G. Karwasz, and E. Illenberger, Eur. Phys. J. D **35**, 417 (2005).

[15] J. Tennyson, J. Phys. B: At. Mol. Opt. Phys. **29**, 6185 (1996).

[16] D. Bouchiha, J. D. Gorfinkiel, L. G. Caron, and L. Sanche, J. Phys. B: At. Mol. Opt. Phys. **40**, 1259 (2007).

[17] A. Jain and K. L. Baluja, Phys. Rev. A **45**, 202 (1992).

[18] L. A. Morgan, J. Tennyson, and C. J. Gillan, Comput. Phys. Commun. **114**, 120 (1998).

[19] P. Pulay, G. Fogarasi, F. Pang, and J. E. Boggs, J. Am. Chem. Soc. **101**, 2550 (1979).

[20] A. A. Sobrinho, L. E. Machado, S. E. Michelin, L. Mu-Tao, and L. M. Brescansin, J. Mol. Struct., Theochem. **539**, 65 (2001).

[21] Q. Sun, C. Winstead, V. Mckoy, J. S. E. Germano, and M. A. P. Lima, Phys. Rev. A **46**, 2462 (1992).

[22] S. Kaur and K. L. Baluja, J. Phys. B: At. Mol. Opt. Phys. **38**, 3917 (2005).

[23] J. N. Shoolery and A. H. Sharbaugh, Phys. Rev. **82**, 95 (1951).

[24] National Institute of Standards and Technology Website: [http://srdata.nist.gov/cccbdb]

[25] S. D. Peyerimhoff, R. J. Buenker, W. E. Kammer, and H. Hsu, Chem. Phys. Lett. **8**, 129 (1971).

[26] D. L. Yeager and V. McKoy, J. Chem. Phys. **60**, 2714 (1974).

[27] T. N. Rescigno, I. I. I. Lengsfield, H. Byron, and C. W. McCurdy, Phys. Rev. A **41**, 2462 (1990).

[28] F. Holtberg, B. Post, and I. Fankuchen, Acta Cryst. **6**, 127 (1953).

[29] F. A. Gianturco and R. R. Lucchese, New J. Phys. **6**, 66 (2004).

[30] A. Jain and K. L. Baluja, Phys. Rev. A **45**, 202 (1992).

[31] A. Jain, Phys. Rev. A **34**, 3707 (1986).

[32] H. L. Cox and R. A. Bonham, J. Chem. Phys. **47**, 2599 (1967).

[33] S. Hara, J. Phys. Soc. Jpn. **22**, 710 (1967).

[34] X. Zhang, J. Sun, and Y. Liu, J. Phys. B: At. Mol. Opt. Phys. **25**, 1893 (1992).

[35] R. Lide, *CRC Handbook of Chemistry and Physics* (CRC Press, Boca Raton, FL, 2003).

[36] G. Staszewska, D. W. Schwenke, D. Thirumalai, and D. G. Truhlar, Phys. Rev. A **28**, 2740 (1983).

[37] C. J. Joachain, *Quantum Collision Theory* (North-Holland, Amsterdam, 1983).

[38] M. Vinodkumar, K. Korot, and H. Bhutadia, Int. J. Mass Spectrom. **294**, 54 (2010).

[39] M. Vinodkumar, C. G. Limbachiya, K. N. Joshipura, and N. J. Mason, Eur. Phys. J. D **61**, 579 (2011).

[40] C. Limbachiya, M. Vinodkumar, and Nigel Mason, Phys. Rev A **83**, 042708 (2011).